ISSN 2176-5480

22nd International Congress of Mechanical Engineering (COBEM 2013)
November 3-7, 2013, Ribeirão Preto, SP, Brazil

COMPARATIVE ANALYSIS FOR GLAZED AND UNGLAZED COLLECTOR FOR USED IN SOLAR DOMESTIC HOT WATERSYSTEMS

Daiane Mieko Iceri
Santiago Del Rio Oliveira
Vicente Luiz Scalon
Departamento de Engenharia Mecânica - UNESP/FE
Av. Luis Edmundo Carrijo Coube, 14-01, Vargem Limpa – CEP: 17033-360, Bauru(SP)
daiane_iceri@hotmail.santiago@feb.unesp.br, scalon@feb.unesp.br

Abstract. *The Solar Domestic Hot Water Systems (SDHWS) coupled to a complementary electric system has being increasingly used. However, it is fundamental a correct design for desired application, unlike advantages will not be verified. There are several methods for designing solar heating systems that calculates useful incident energy on the collector, but one widely used considers only the parcel above of critical radiation as useful energy and a minimum operation temperature is known. This procedure is usually denominated as ϕ, f-Chart Method. This methodology considers a closed solar water heating system with no restrictions about the collector inlet temperature, but it takes account a minimum discharge temperature . The ϕ, f-Chart Method combines the Utilizability Method, that obtains the minimum rate from a monthly average daily critical radiation incident on the collector, which occurs when the load temperature is minimal with the f-Chart Method. This combination of methods allows obtaining the maximum efficiency for the system using the dimensionless parameters from f-Chart Method. This study will compare two solar heating systems: a glazed collector with single cover and an unglazed one. The main parameter evaluated is the solar fraction, that supplies the hot water demand and the absorbed useful energy. This study is developed for the climatic conditions of Bauru city and uses a computational routine of the Method ϕ, f-Chart developed on GNU-Octave for designing the solar heating system. Comparing the results of both devices one can determine the differences on electric energy consumption of each one.*

Keywords: *ϕ-f-Chart Method, Solar Domestic Hot Water, Solar Energy*

1. INTRODUCTION

Several crises in the past remember the great world dependence for using oil as a main power supply. Environmental risk of degradation have been more apparent. Research for improvement and replacement technologies by alternative sources became an important topic for life preservation on the planet. Beyond that, renewable energy resources seems the most efficient and effective solutions (Kalogirou, 2004). The combined use of renewable energy shows the great importance in reducing residential energy consumption, significantly. Thus, Solar Domestic Hot Water Systems(SDHWS) could be seemed on houses roofs what showing its once a well design system will reduce significantly the electricity demand in residences at peak periods.

The Solar Domestic Hot Water Systems is basically composed by a flat plate solar collector, a boiler and by an auxiliary heating system, as shown in Fig. 1. Solar collectors are able to transform solar radiation into useful energy increasing water temperature as it flows through the collector. According to Kalogirou (2004), the flat plate collectors are most appropriate for obtaining hot water for residential system and consist by a transparent cover, usually glass, a heat absorbing black surface, pipes and an insulated box, as shown in Fig. 2 Lima (2003) quotes advantages from flat plate collectors with respect to other types are: construction simplicity, low cost, no moving parts, ease to maintain and durability. The flat plate solar collectors can absorb direct, diffuse and reflected solar radiation. Thus, they can be fixed on residences roofs with no monitoring systems for sun movement and only needs to be placed facing the equator.

The cover on the collectors is used to reduce convection heat losses to the environment and prevents radiation losses from the absorbing surface. This changes in radiation energy creates the "greenhouse effect" in the collector, increasing the energy that remains inside the collector (Souza, 2009). However, the glass cover also increases thermal radiation reflection on surface and, consequently, also contributes for reducing useful energy. The unglazed flat plate collectors could be used when temperature demand is low, once it is a system with large heat losses to atmosphere, mainly by forced convection. However, this system is cheaper than covered one and it is usually used for heating pools water. Heated water should be stored in the storage tank for maintaining required temperature until the time to be used, that are often on evenings or nighttime. At this time, if the water temperature on the reservoir is low, an auxiliary heating system needs to be used for completing the required demand.

There are several types of solar water heating systems and they basically vary in materials used on collectors manufacturing, which influences significantly on the performance of system. Maximum useful energy absorbed by fluid for heating water occurs when the plate has a high absorption and low emissivity for re-irradiation and it is covered. These characteristics depend on the material quality selected for coating the collector. Furthermore, the collector plate

ISSN 2176-5480

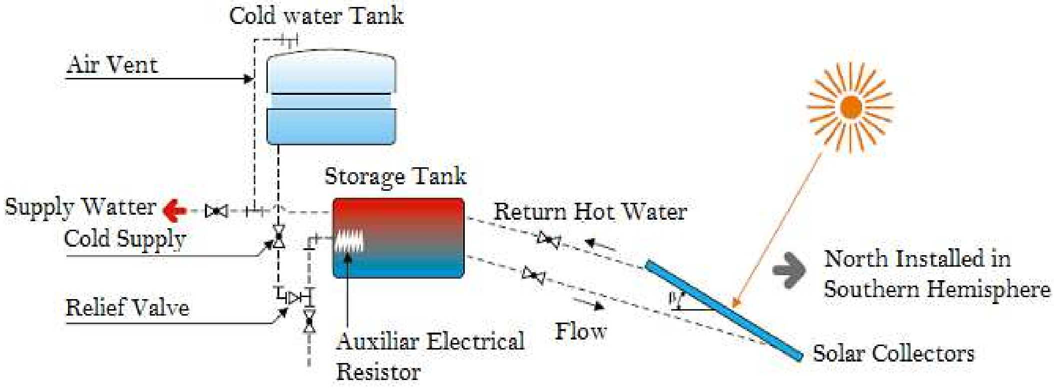

Figure 1. Scheme of Solar Domestic Hot Water Systems installation (Lima, 2003)

absorptance is very important and it depends on the absorber surface color and the inclination angle of collector. Usually, the color most used in surfaces is black, and an inclination angle is the latitude plus ten degrees (Kalougirou,2004).

Typically water circulation system on SDHWS occurs by natural circulation in a phenomena knew as thermosyphon effect. In this phenomena, at same time that water increases its temperature it reduces its density causing a thrust effect that pushes water from the collector into the reservoir and, consequently, the water recirculation.

Cole *et al.*. (2008) defined the solar fraction as the ratio of solar-supplied energy to total thermal load and it is dependent on available solar radiation, collector efficiency, collector surface area and thermal load. Therefore, it is necessary to develop methodologies for determining the solar fraction on a solar heat system. So, according to Azad (2012), the F-chart method was used to estimate the fraction of the monthly hot water load that was provided by solar energy. The method, developed by Klein and Beckman (1979), was known as ϕ, f-Chart and it was developed for designing solar heating systems. Using this procedure, it is possible to calculate solar fraction that contributes for heating water according to meteorological data characteristics for location and installed system. The method considers yet a closed system, as shown in Fig. 3, with no restrictions for inlet temperature on the collector, although the temperature discharge needs to be greater then a minimum value.

This method considers only radiation above the critical is useful, as well as the Daily Utilizability Method and the dimensionless parameters like f-Chart Method to define the fraction of the solar system is able to supply. According to Hazel and Langevine (1994), the solar collector maximum utilizability ϕ is defined the fraction of the incident radiation that can be converted into useful heat by having the collector $F_R(\tau\alpha)$ is 1, which F_R is the collector heat removal factor and $\tau\alpha$ is the effective transmittance absorptance product of the collector cover, and operating at a fixed temperature difference for the ambient temperature and the collector inlet temperature. Using the f-Chart Method, ϕ *and* f-Chart, one can calculate the energy fraction that the solar system is capable to supply. From dimensionless parameters it is possible to obtain the percentage solar radiation will provide and also obtain the amount of auxiliary energy is needed to complete the demand.

This study will analyze different Solar Domestic Hot Water Systems, considering the unglazed collector, single glazed and double glazed. Furthermore, it will analyze different efficiencies for collectors simple glazed and unglazed collectors according to the classification of the National Institute of Metrology, Quality and Technology (INMETRO,1993). The procedure is based on the monthly energy production specific per unit area for each collector converted in useful energy. The monthly average hourly radiation incident data and the average temperature are considered from Bauru city and obtained by website Sociedade do Sol (2003), which presents the radiation for the typical days for each month. It designed a routine on GNU-Octave to estimated solar fraction for typical days, for each

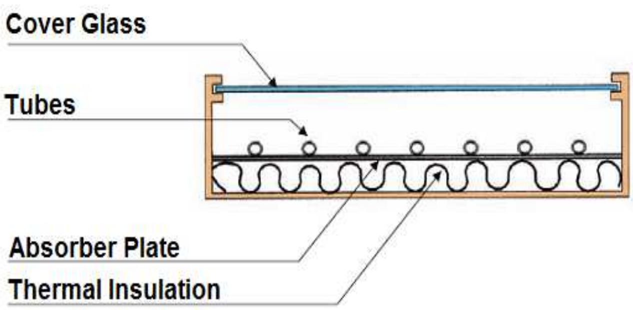

Figure 2. Components of a flat plate solar collector (Arruda, 2004)

ISSN 2176-5480

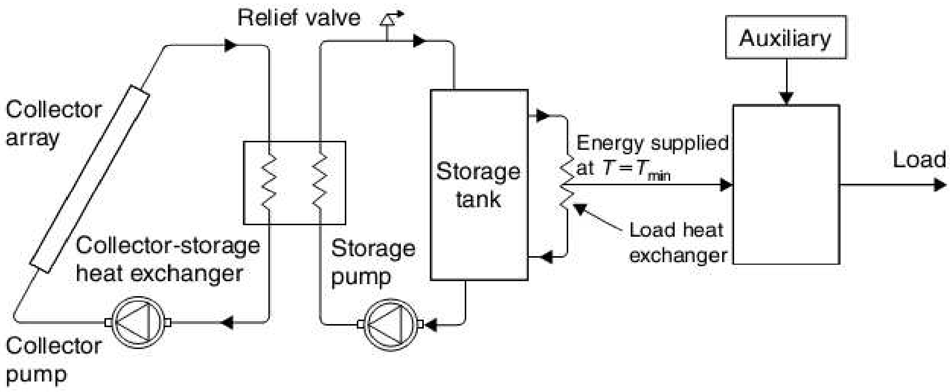

Figure 3. Closed system considered for the ϕ, f-Chart Method (Kalogirou, 2009)

month, during a year, based on the ϕ, f-Chart Method. The expected result is to obtain lower fractions solar for smaller efficiencies system, especially for cooler times of the year, since the heat losses to the environment will be greater.

2. METHODOLOGY

The ϕ,f-Chart Method is based on the f-Chart Method, both define the non-dimensional parameters X and Y for obtaining the monthly solar fraction. These parameters are basically dependent on the collector characteristics: collector area, boiler coefficient of heat loss collector (U_L), heat removal factor (FR) transmittance-absorptance products ($\tau\alpha$), total solar radiation on the collector plate, demand to be supplied and maximum daily utilizability to one system. But this methodology could do correction in the dimensionless parameter that represents the ratio of the total solar energy absorbed to the total heating load or demand during the same period (Y) based on the Daily Utilizability Method. Thus, procedures such calculations are presented in the following sections.

2.1 Ratio of the monthly average beam radiation on a tilted surface to that on a horizontal surface. ($\bar{R}_B$)

The R_B ratio is a complex function of atmospheric transmittance and Liu and Jordan (1963) determined that can possible to calculate a factor by the ratio of the extraterrestrial radiation on a tilted surface and on a horizontal surface for month, for surfaces facing directly towards the equator, and given by Eq. (1) for the Northern Hemisphere and Eq. (2) for the Southern Hemisphere.

$$\bar{R}_B = \frac{\cos(L-\beta)\cdot\cos(\delta)\cdot\sin(\mathrm{hss}')+(\pi/180)\cdot\mathrm{hss}'\cdot\sin(L-\beta)\cdot sen(\delta)}{\cos(L)\cdot\cos(\delta)\cdot\sin(\mathrm{hss})+(\pi/180)\cdot\mathrm{hss}\cdot\sin(L)\cdot\sin(\delta)} \tag{1}$$

$$\bar{R}_B = \frac{\cos(L+\beta)\cdot\cos(\delta)\cdot\sin(\mathrm{hss}')+(\pi/180)\cdot\mathrm{hss}'\cdot\sin(L+\beta)\cdot\sin(\delta)}{\cos(L)\cdot\cos(\delta)\cdot\sin(\mathrm{hss})+(\pi/180)\cdot\mathrm{hss}\cdot\sin(L)\cdot\sin(\delta)} \tag{2}$$

2.2 Ratio of hourly total radiation to daily total radiation at noon (h=0°) (r_n)

To predict the performance of solar heating systems, hourly radiation value are needed, but these data are not generally available. But it can get from radiation daily average, over the long term, through empirical correlations. According Collares-Pereira and Rabl (1979b) an empirical relationship for rn is defined by Eq. (3)

$$r_n = \frac{\pi}{24}(\alpha+\gamma\cdot\cos(h))\frac{\cos(h)-\cos(\mathrm{hss})}{\sin(\mathrm{hss})-((2\cdot\pi\cdot\mathrm{hss})/360)\cdot\cos(\mathrm{hss})} \tag{3}$$

which:

$$\alpha = 0.409+0.5016\cdot\sin(\mathrm{hss}-60) \tag{4}$$

$$\gamma = 0.6609-0.4767\cdot\sin(\mathrm{hss}-60) \tag{5}$$

2.3 Ratio of hourly diffuse radiation to daily diffuse radiation at noon (h=0°) ($r_{d,n}$)

Liu and Jordan (1977) also defined the empirical correlation rd, n, in order to obtain the average diffuse radiation at noon through daily data, represented by Eq. (6):

$$r_{d,n}=\frac{\pi}{24}\frac{\cos(h)-\cos(\text{hss})}{\sin(\text{hss})-((2\cdot\pi\,\text{hss})/360)\cos(\text{hss})} \tag{6}$$

2.4 Beam radiation tilt factor at noon (h=0°) ($R_{B,n}$)

The radiation data measured on a horizontal surface, but in practice it used tilted collectors. The inclination of solar collectors varies according to its application and it is generally used an inclination angle ten degrees more the site latitude and facing to equator. Thus, the RB factor was estimated to convert the direct radiation on a horizontal surface to a tilted surface.

For collector face to South, or installed in the Northern Hemisphere RB is given by:

$$R_{B,n}=\frac{\cos(\theta)}{\cos(\Phi)}=\frac{\sin(L-\beta)\cdot\sin(\delta)+\cos(L-\beta)\cdot\cos(\delta)\cdot\cos(h)}{\sin(L)\cdot\sin(\delta)+\cos(L)\cdot\cos(\delta)\cdot\cos(h)} \tag{7}$$

For collector face to North, or installed in the Southern Hemisphere RB is given by:

$$R_{B,n}=\frac{\cos(\theta)}{\cos(\Phi)}=\frac{\sin(L+\beta)\cdot\sin(\delta)+\cos(L+\beta)\cdot\cos(\delta)\cdot\cos(h)}{\sin(L)\cdot\sin(\delta)+\cos(L)\cdot\cos(\delta)\cdot\cos(h)} \tag{8}$$

2.5 Monthly total radiation tilt factor ($\bar{R}$)

It is defined as the ratio of the average monthly total radiation on an inclined surface ($\bar{H}_t$) and the monthly average total radiation and $\bar{R}$ can be defined as:

$$\bar{R}=\frac{\bar{H}_t}{\bar{H}}=(1-\frac{\bar{H}_D}{\bar{H}})\cdot\bar{R}_B+\frac{\bar{H}_D}{\bar{H}}\cdot[\frac{1+\cos(\beta)}{2}]+\rho_G\cdot[\frac{1-\cos(\beta)}{2}] \tag{9}$$

2.6 Ratio for the hour centered at noon of radiation on the tilted surface to that on a horizontal surface for an average day of the month (Rn)

Equation (10) shows the conversion factor for radiation at noon on a surface inclined relative to a horizontal surface according to an interest day.

$$R_n=(\frac{I_t}{I})_n=(1-\frac{r_{d,n}\cdot H_D}{r_n})\cdot R_B,n+(\frac{r_{d,n}\cdot H_D}{r_n H})[\frac{1+\cos(\beta)}{2}]+\rho_G\cdot[\frac{1-\cos(\beta)}{2}] \tag{10}$$

2.7 Transmittance-Absorptance product ($\tau\alpha$)

The absorptance transmittance product of collector depends on the material it is made and the angle of incidence of solar radiation, but direct, diffused and reflected radiation focus with a different angle, for the same instant. The monthly average transmittance-absorptance product ($\tau\alpha$) is equal to the ratio between average radiation absorbed by the average radiation incident on the collector.

$$\bar{\tau\alpha}=\frac{\bar{S}}{\bar{H}_t} \tag{11}$$

The radiation absorbed by the collector is given by Eq. (12).

$$\bar{S}=\bar{H}_B\cdot\bar{R}_B\cdot(\bar{\tau\alpha})_B+\bar{H}_D\cdot(\bar{\tau\alpha})_D\cdot[\frac{1+\cos(\beta)}{2}]+\bar{H}\cdot\rho_G\cdot(\bar{\tau\alpha})_G\cdot[\frac{1-\cos(\beta)}{2}] \tag{12}$$

Substituting equation (12) in the (11) and the dividing by transmittance-absorptance product normal to the surface, obtained:

ISSN 2176-5480

$$\frac{(\bar{\tau\alpha})}{(\tau\alpha)_n}=\frac{\bar{H}_B}{\bar{H}_t}\cdot\bar{R}_B\cdot\frac{(\bar{\tau\alpha})_B}{(\tau\alpha)_n}+\frac{\bar{H}_D}{\bar{H}_t}\cdot\frac{(\bar{\tau\alpha})_D}{(\tau\alpha)_n}\cdot[\frac{1+\cos(\beta)}{2}]+\frac{\bar{H}}{\bar{H}_t}\cdot\rho_G\cdot\frac{(\bar{\tau\alpha})_G}{(\tau\alpha)_n}\cdot[\frac{1-\cos(\beta)}{2}] \tag{13}$$

Thus, the ratios between the transmittance-absorptance products for each radiation need to be obtained. The angles of incidence for radiation reflected (Eq. (14)) and diffused (Eq. (15)) were determined by Brandemuehl and Beckman (1980), and the beam radiation angle is equal to tilted angle.

$$\theta_{e,G}=90-0{,}5788\cdot\beta+0{,}002693\cdot\beta^2 \tag{14}$$

$$\theta_{e,D}=59{,}68-0{,}1388\cdot\beta+0{,}001497\cdot\beta^2 \tag{15}$$

Klein (1979) defined the graph shown in Fig. 4, which shows the relation between the angle of incidence to collector with 1 to 4 covers. From these graph Kalogirou (2009) found an approximate equation for collectors with single (Eq. (16)) and double (Eq. (17)) coverage. Both definition graph as the equations shown below were considered a reflectivity of 1.526.

$$\frac{(\bar{\tau\alpha})}{(\tau\alpha)_n}=-8{,}7\times10^{-8}\cdot\theta^4+1{,}03\times10^{-5}\cdot\theta^3-0{,}0004762\cdot\theta^2+0{,}00851\cdot\theta+0{,}94967 \tag{16}$$

$$\frac{(\bar{\tau\alpha})}{(\tau\alpha)_n}=-5{,}05\times10^{-8}\cdot\theta^4+3{,}578\times10^{-6}\cdot\theta^3-8{,}777\times10^{-5}\cdot\theta^2-1{,}836\times10^{-6}\cdot\theta+1{,}0042 \tag{17}$$

2.8 ϕ, *f*-Chart parameters

Initially it is necessary to define the hot water demand, considering the sense of 2010, the average number of persons per residence is 3.34, so it was adopted for the project an amount of 4 people per house. According to the solar collectors manufacturer, Soletrol, for a comfortable bath, the flow of shower must be from 4 to 6 liters per minute as shown in Tab. 1. Furthermore, it was estimated by the same producer, the average time for bath per person daily is 10 minutes. Thus, a person consumes 50 liters daily for bathing, taking into account the residence with 4 people, it will need 200 liters of hot water per day.

Defined the hot water demand Q_L as 200 liters per day, it is possible to calculate the daily energy demand for the study residency, by Eq. (18).

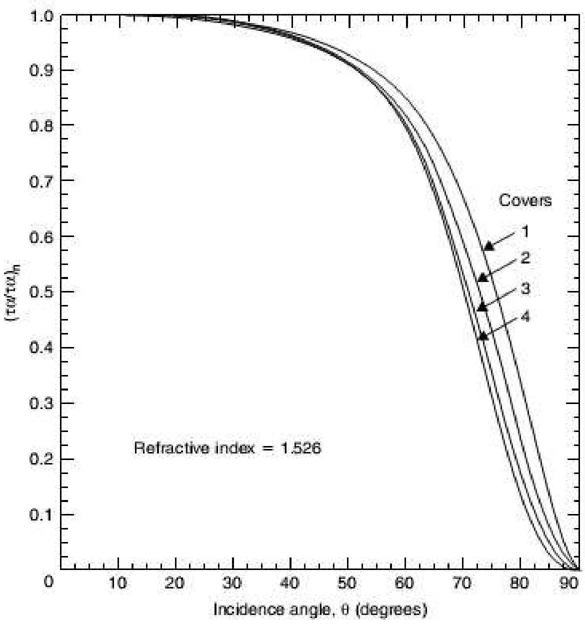

Figure 4. Relationship between transmittance-absorptance product and incidence angle (Kalogirou, 2009)

$$L = Q_L \cdot n \cdot c_p \cdot (T_L - Taf) \tag{18}$$

Table 1. Comfort bath to showers flows

Operating showers ranges	Operating conditions and bath comfort
Equal or lower than 3 liters per minute	Extremely uncomfortable and it is proportional to the electric showers with very low electrical power.
3 to 4 liters per minute	Reduced comfort. It is the standard flow of the great majority of electric showers which electrical powers are between 4,400 watts and 5,000 watts.
4 to 5 liters per minute	Considered reasonable. This flow provides a little more comfort and it is obtained by passing heaters with large power
5 to 6 liters per minute	Good comfort. It is the normal flow to be adopted in residential applications.
6 to 8 liters per minute	Great comfort. This flow range provides a very comfortable shower without wasting water.
8 to 10 liters per minute	Excellent comfort. As in the previous case, flows are comfortable and acceptable. However, the design of the heating system begins to reach high volumes.
Above 10 liters per minute	Excessive, it characterized in waste water and in some cases exceeding the limit of comfort. In many situations this flow damages the solar heating efficiency.

To calculate the maximum daily utilizabity for the system is necessary to define the dimensionless parameter Xc, the minimum dimensionless critical radiation level which is the ratio of the radiation average monthly minimum critical incident by the radiation at noon for a typical day of the month. The maximum energy absorbed by the collector occurs when radiation on it is the minimal critical radiation and the maximum radiation over it, which occurs at noon, so the load temperature is minimal.

$$\bar{X}_{C,min} = \frac{\dfrac{F_R U_L \cdot (T_{min} - \bar{T}_a)}{F_R (\bar{\tau\alpha})}}{r_n \cdot R_n \cdot \bar{K}_t \cdot \bar{H}_0} = \frac{\dfrac{F_R U_L \cdot (T_{min} - \bar{T}_a)}{F_R (\tau\alpha)_n \cdot (\bar{\tau\alpha})/(\tau\alpha)_n}}{r_n \cdot R_n \cdot \bar{K}_t \cdot \bar{H}_0} \tag{19}$$

Estimated the dimensionless parameter critical radiation is possible to obtain the maximum daily utilizability:

$$\bar{\phi}_{max} = \exp[(A + B \times \frac{R_n}{\bar{R}})(\bar{X}_{C,min} + C \cdot \bar{X}^2_{C,min})] \tag{20}$$

Which:

$$A = 2{,}943 - 9{,}271 \cdot \bar{K}_t + 4{,}031 \cdot \bar{K} t^2$$
$$B = -4{,}345 + 8{,}853 \cdot \bar{K}_t - 3{,}602 \cdot \bar{K}_t^2$$
$$C = -0{,}170 - 0{,}306 \cdot \bar{K}_t + 2{,}936 \cdot \bar{K}_t^2$$

The parameters used by the f-Chart method are calculated the same way:

$$\bar{\phi}_{max} Y = \bar{\phi}_{max} \frac{A_c \cdot F_R (\bar{\tau\alpha}) \cdot N \cdot \bar{H}_t}{L} \tag{21}$$

$$X' = \frac{A_c \cdot F_R U_L \cdot (100) \cdot \Delta t}{L} \tag{22}$$

The correction parameter for the boiler Rs, which is the ratio of standard storage heat capacity per unit of collector area of 350 kJ/m2-°C to actual storage capacity is given by Klein and Beckman (1979).

$$R_s = \frac{350}{\dfrac{Mc_p}{A_c}} \tag{23}$$

ISSN 2176-5480

Finally, the solar fraction which is the monthly total load supplied by a standard solar liquid-based solar energy is calculated on the basis of typical days for each month by analytical equation, defined by Klein and Beckman (1979) given by Eq. (24).

$$f = \bar{\phi}_{max} Y - 0{,}015 \cdot [\exp(3{,}85 \cdot f) - 1][1 - \exp(-0{,}15 \cdot X')] R_s^{0{,}76} \quad (24)$$

3. RESULTS AND DISCUSSION

According the methodology presented above, it was possible to develop a computational routine on GNU-Octave. The Bauru(SP) climatic conditions were considered with data obtained from the Sociedade do Sol (2003) which aims to develop activities related to the environment. Table 2 presents specifications for standard collectors, unglazed, simple glazed and double glazed. The same conditions were considered for calculating solar fraction in all the cases evaluated. The main information used for these applications was shown in Tab. 3. Thus, the solar fraction could be obtained over a year for this region, as can be seen in Fig. 5.

Table 2. Coefficient of heat loss collector-heat removal factor product and heat removal factor-transmittance and absorptance product (Kalogirou, 2009)

Collector	Fr(τα)n	FrUL
Unglazed	0.975	20.313
Simple Glazed	0.845	8.833
Double Glazed	0.787	5.957

In Figure 5, one can observe that on warm seasons, spring and summer, the differences between the solar fractions are small. This fact contrasts with cold seasons, where low surroundings temperature increases heat losses. So, in this situation the solar fraction for an unglazed collector is lower.

Table 3. Specifications for the applied system

Hot Water Demand	Collector Area	Storage Tank Volume	Tilt Angle	Minimum Temperature	Average Cold Water Temperature	Supply Temperature	Solar Constant
200 L	2 m2	200 L	30°	30°	15°	60°	1366,1

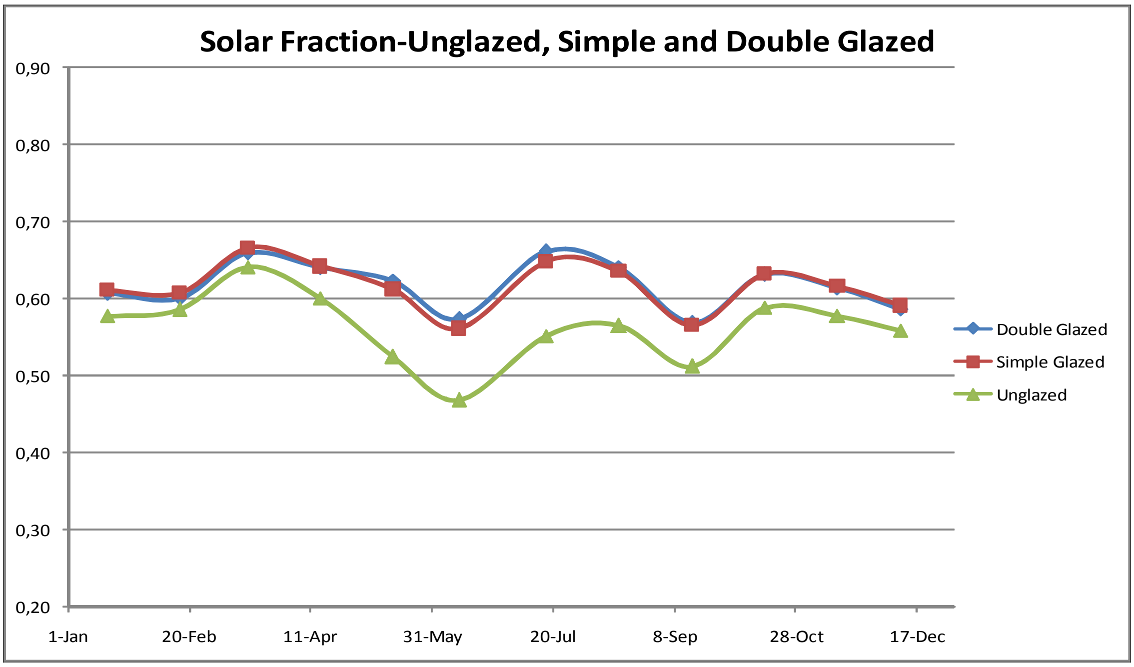

Figure 5. Diagram of solar fraction over a year for unglazed, simple glazed and double glazed collectors

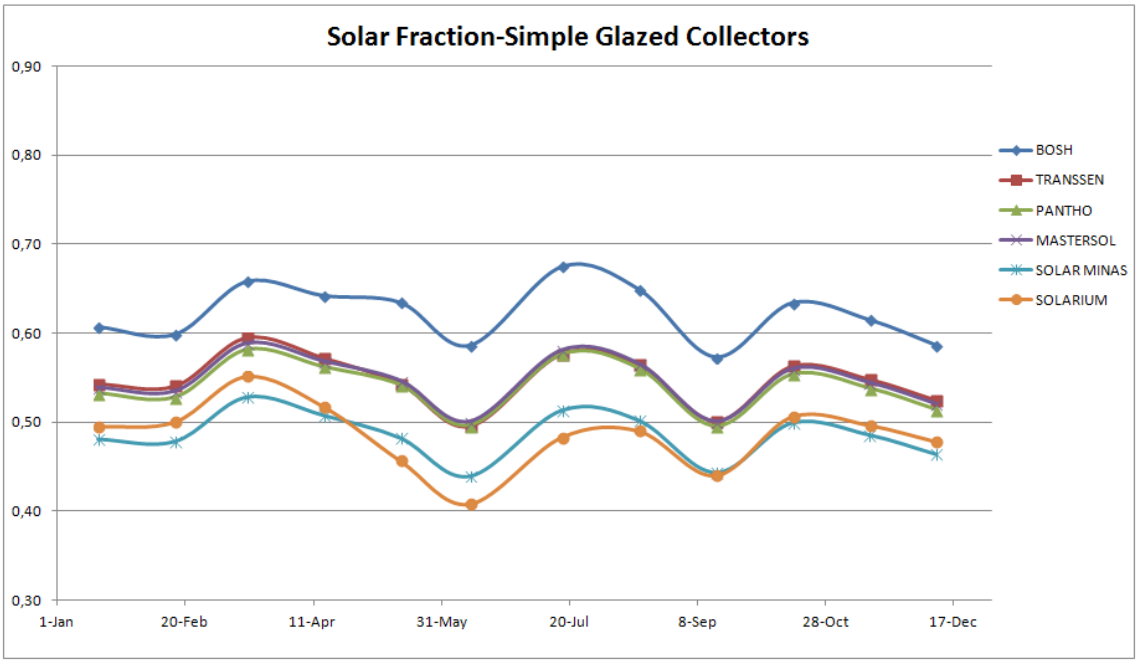

Figure 6. Diagram of solar fraction over a year for standard simple glazed collectors

Table 4 shows INMETRO (1993) classification considering the average monthly energy supply, and each specification for each simple glazed collector. From its characteristics, it was possible to obtain Fig. 6, which shows the solar fractions for each producer assuming the local radiation. Figure 6 shows glazed collectors of different energy efficiencies, which are classified as A for better efficiencies, to C, for the lower efficiencies. It is possible to verify that all collector with the similar efficiencies have equivalent performance over the year and independent of season.

Table 4. Specifications for standard simple glazed collectors (INMETRO, 1993)

Producer	Average Monthly Energy Supply [kWh/month.m^2]	Classification	Material	Fr(τα)n	FrUL
BOSH	90	A	Aluminum	0.75	4.03
TRANSSEN	77.5	A	Polypropylene	0.741	7.969
PANTHO	76.2	B	Copper	0.695	6.054
MASTERSOL	76	B	Aluminum	0.71	6.467
SOLAR MINAS	64.2	C	Aluminum	0.642	6.7
SOLARIUM	61.9	C	Thermoplastic	0.78	14.726

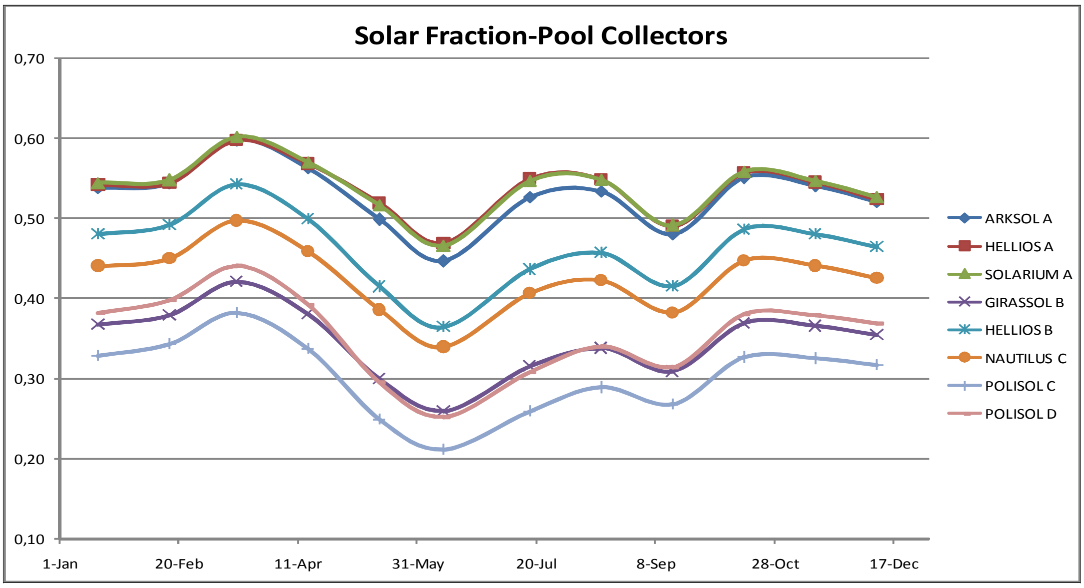

Figure 7. Diagram of solar fraction over a year for unglazed collectors

Table 5 presented different unglazed collectors that are used for heating water for swimming pool based on INMETRO (1993) information. In this report collectors are classified from A to D(the higher to the lowest), in the same way that glazed collectors according with average monthly energy supply per area. It is possible to observe in Fig. 7 that the collectors for swimming pool have lower solar fraction once they have higher heat losses than the glazed one. The $F_R\ U_L$ factor is the most significant parameter for analyzing heat losses by convection to the environmental it has important decrease when cover is present.

Table 5. Specifications for unglazed collectors (INMETRO, 1993)

Producer	Average Monthly Energy Supply [kWh/month.m^2]	Classification	Material	Fr(τα)n	FrUL
ARKSOL	102.4	A	EPDM [(1)]	0.86	16.16
HELLIOS	100.3	A	Polypropylene	0.81	12.46
SOLARIUM	99.1	A	Thermoplastic	0.83	13.54
GIRASSOL	91.3	B	Polymer	0.66	18.58
HELLIOS	94.9	B	Polypropylene	0.84	20.72
NAUTILUS	84.6	C	Polyethylene	0.74	17.22
POLISOL	83.8	C	Black Polypropylene	0.76	21.22
POLISOL	73.3	D	Polypropylene	0.74	23.72

[(1)] ethylene-propylene-diene rubber with saturated chain

Considering the collector major energy efficiency on Tab. 4 and the same characteristics for the system previous applied, presented in Tab. 3, and the data of radiation from the Sociedade do Sol (2003) for the cities of Bauru, Rio de Janeiro and São Paulo, given in Tab. 6, it was possible to obtain the solar fractions for all cities over a year, as shown in Fig. 8. Most of solar fractions are higher in the city of Bauru, followed by Rio de Janeiro and São Paulo, respectively. However, in January, February and May the solar fractions of Rio de Janeiro are higher than Bauru. This phenomenon is verified because radiation on first city are lower than the second one and also surroundings temperatures for those months are higher in Rio de Janeiro. The solar fractions for São Paulo are lower for the other two cities in about 20%, which is caused by the smaller radiation shown in Tab. 6.

Table 6. Radiation and solar fraction for the cities of Bauru, Rio de Janeiro and São Paulo (Sociedade do Sol, 2003)

Day/Month	BAURU		RIO DE JANEIRO		SÃO PAULO	
	Solar Fraction	Radiation [kWh/m^2]	Solar Fraction	Radiation [kWh/m^2]	Solar Fraction	Radiation [kWh/m^2]
17/Jan	0.6073	5.97	0.6113	5.86	0.4142	4.25
16/Feb	0.5987	5.44	0.6362	5.67	0.5295	5.00
16/Mar	0.6583	5.42	0.6420	5.22	0.4576	4.06
15/Apr	0.6424	4.72	0.5450	4.06	0.4409	3.61
15/May	0.6347	4.25	0.7652	4.83	0.4200	3.19
11/Jun	0.5861	3.69	0.5053	3.22	0.4122	2.94
17/Jul	0.6750	4.25	0.5950	3.78	0.4473	3.22
16/Aug	0.6498	4.61	0.5607	4.06	0.4710	3.72
15/Sep	0.5731	4.67	0.5078	4.22	0.4112	3.75
15/Oct	0.6344	5.69	0.5332	4.86	0.4050	4.03
14/Nov	0.6152	5.97	0.5443	5.28	0.4865	5.00
10/Dec	0.5867	5.86	0.5684	5.61	0.4287	4.53

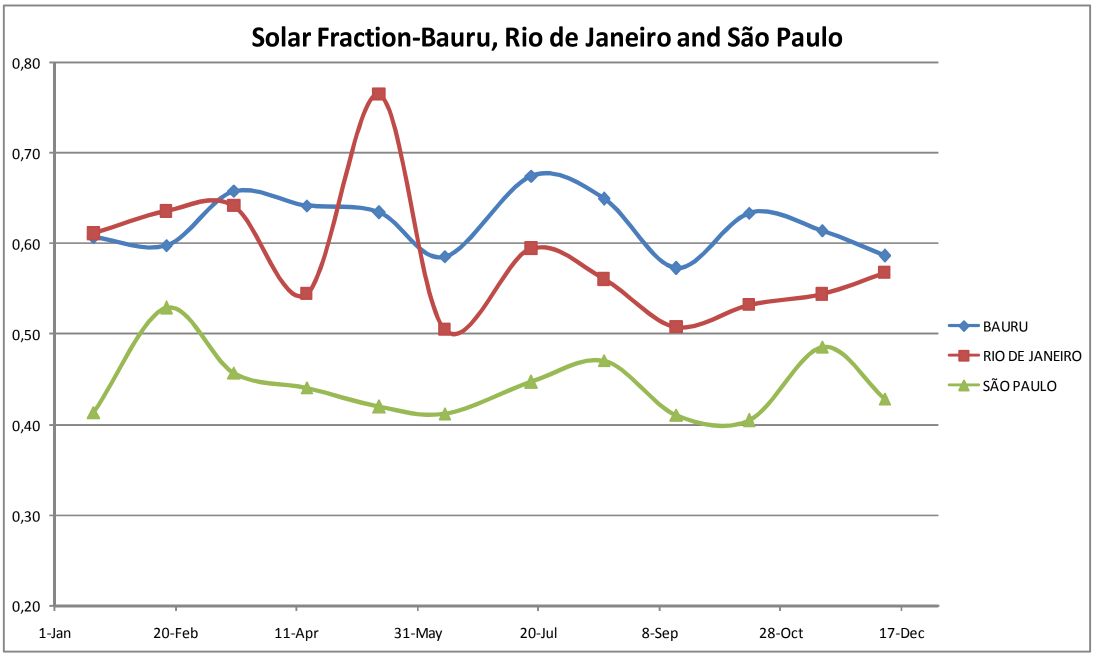

Figure 8. Diagram of Solar Fraction over a year for Bauru, Rio de Janeiro and São Paulo for high efficiency collector

4. CONCLUSIONS

Based on the results presented, it is possible to observe collectors with different efficiency, glazed or unglazed, have similar behaviors. For Bauru, radiation difference for single and double coverage is not significant, so double glass is not interesting to application. Comparing unglazed collectors and simple glazed, differences in solar fractions during cold seasons are more significant, and even 10%.

From Figure 6, it can be seen that solar collectors with simple cover are quite similar ways in each collectors classes. In other words, for the same efficiency, collectors have close values solar fractions. Considering small variations due to collector material with plates made of metals, such as copper and aluminum, have more heat loss. This fact is due to these plates operates on higher temperatures then other materials, such as thermoplastic. It is noticeable low efficiency for some of these solar collectors. In the months from January to April and from October to December the solar fraction

ISSN 2176-5480

is higher for the thermoplastics ones and the other months of the year the aluminum one have a higher solar fraction.

Unglazed collectors, used for heating swimming pools, have almost the same performance throughout the year according to their efficiency, since which have higher efficiencies are those have the higher solar fractions and which have lower efficiency the solar fractions is lower, as shown in Fig. 7. The solar fraction for unglazed collectors are much smaller than those of single coverage, for bath collectors, the solar fractions range from 0.8 to 0.4 and used for pool heating, varies between 0.6 and 0.2.

Considering the high efficiency solar collector for bath, installed in the Bauru, Rio de Janeiro and São Paulo, the solar fraction, as shown by Fig. 8. This parameter is higher for Bauru during most of the year and after Rio de Janeiro and São Paulo, respectively. In February and May, the solar fraction to Rio de Janeiro outperforms Bauru, because its radiation is higher. Already the solar fractions for São Paulo are much lower for the other two cities, throughout the year and, sometimes reaches 0.23. This happens because São Paulo has lower levels of radiation, as can be seen in Tab. 6. Presence of atmospheric pollution and the urbanization block sunlight and lower surrounding temperatures leads the solar collectors to greater heat loss by convection.

5. ACKNOWLEDGEMENTS

The authors wish thank to CAPES, for financial support to the MSc. student Daiane Mieko Iceri.

6. REFERENCES

Arruda, L. B., 2004. *Operação de sistemas de aquecimento solar de água com controle de vazões em coletores planos*. Ph.D. thesis, Escola Politécnica, University of São Paulo, São Paulo.

Azad, E., 2012. "Design installation and operation of a solar thermal public bath in eastern Iran". *Energy for Sustainable Development*, Vol. 16, p. 68-73.

Brandemuehl, M. and Beckman, W., 1980. "Transmission of diffuse radiation through cpc and flat plate collector glazings", Solar Energy, Vol. 24, p. 511-513.

Cole, S., Pereira, G.S., Vidal Gutiérrez, H.R., Escobar Moragas, R., 2009. "On the validity of a design method for a solar-assisted ejector colling system". *Solar Energy*, Vol. 83, p. 139-149.

Collares-Pereira, M. and Rabl, A., 1979a. "Derivation of method for predicting long term average energy delivery of solar collectors". Solar Energy, Vol. 23, p. 223-233.

Collares-Pereira, M. and Rabl, A., 1979b. "The average distribuition of solar radiation – correlations between diffuse and hemispherical and between daily and hourly insolation values", Solar Energy, Vol. 22, p. 155-169.

Hazel, R.D. and Langevine, L.P., 1994. "Flat plate collector utilizability for Guyana". *Renewable Energy*, Vol. 4, p. 437-439.

Instituto Brasileiro de Geografia e Estatística, 1993. “Caracterização da população e dos domicilios”. 11 Apr. 2013 <http://biblioteca.ibge.gov.br/visualizacao/periodicos/93/cd_2010_caracteristicas_populacao_domicilios.pdf >

Instituto Nacional de Metrologia, Qualidade e Tecnologia, 1993. “Tabelas de consumo/eficiência energética”. 20 Apr. 2013 <http://www.inmetro.gov.br/consumidor/tabelas.asp>.

Kalogirou, S.A., 2009. *Solar Energy Engineering*. Elsevier, San Diego. 1st edition.

Kalogirou, S.A., 2004. "Solar thermal collectors and applications". Progress in Energy and Combustion Science, Vol. 30, p. 231-295.

Klein, S., 1978. "Calculation of flat-plate collector utilizability". Solar Energy, Vol. 21, p. 393-402.

Klein, S., 1979. "Calculation of the monthly-average transmittance-absorptance product". Solar Energy, Vol. 23, p. 547-551.

Klein, S. and Beckman, W., 1979. "A general design method for closed-loop solar energy systems". Solar Energy, Vol. 22, p. 269-282.

Liu, BY. and Jordan, RC., 1963. "The long-term average performance of flat-plate solar-energy collectors: with design data for the u.s., its outlying possessions and canada". *Solar Energy*, Vol. 7, p. 53-74.

Lima, J.B.A., 2003. *Otimização de sistema de aquecimento solar de água em edificações residenciais unifamiliares utilizando o programa TRNSYS.* Master thesis, Escola Politécnica, University of São Paulo, São Paulo.

Sociedade do Sol, 2003. “Projeto Aquecedor Solar de Baixo Custo”. 20 Apr. 2013 <http://www.sociedadedosol.org.br/dicas/dicas_02.htm>.

de Souza, A.G.L., 2009. *Desenvolvimento de software para projeto de sistemas centralizados de aquecimento solar de água.* Master thesis, State of Rio de Janeiro University, Rio de Janeiro.

Soletrol Aquecedores Solares de Água, 2003. “Técnicas e Instalações”. 10 Apr. 2013 <http://www.soletrol.com.br/noticias/agua_e_sol/09/pg02.php >

7. RESPONSIBILITY NOTICE

The author(s) is (are) the only responsible for the printed material included in this paper.